Numerical simulation of shell-filling effects in circular quantum dots

M. Macucci
Dipartimento di Ingegneria dell'Informazione, Università di Pisa, Via Diotisalvi, 2, I-56126 Pisa, Italy

Karl Hess
Beckman Institute, University of Illinois, 405 North Mathews Avenue, Urbana, Illinois 61801

G. J. Iafrate
U.S. Army Research Office, Research Triangle Park, North Carolina 27709-2211

(Received 15 November 1996)

We have computed the capacitive energy associated with the addition of each electron to a circular quantum dot, reproducing the shell-filling behavior as reported in previous simulations and recently found experimentally. We derived quantitative estimates for the shape of the confining potential and for the dot radius in the experiments. Our results show that the succession of shell-filling events differs for the case of a realistic self-consistent potential from that predicted by a single-electron approximation and with an idealized parabolic potential. [S0163-1829(97)51808-X]

Recent measurements by Tarucha *et al.*,[1] using vertical quantum dots, have provided experimental evidence of the shell structure of addition energies as predicted in Refs. 2–4. This has been possible through a sophisticated technology[5,6] that has allowed the fabrication of smaller and geometrically more controllable quantum dots. The vertical confinement has been obtained with Al_xGaAs_{1-x} barriers 12 nm apart and the lateral confinement by etching and by the deposition of a side gate that can be used to control the dot potential. Tarucha *et al.* devised an improved procedure for the determination of the addition energies from the data of the Coulomb blockade conductance peaks as a function of the gate voltage. A method that was well known in the field of Coulomb blockade studies has been applied, exploiting the information on the slopes in the diamond diagram[7] to evaluate the charging energy from the values of the gate voltage that correspond to conductance peaks.

In this paper, for labeling the addition energies in relationship to the number of electrons in the dot, we use the same convention as in the paper by Tarucha *et al.*, which yields the most direct physical interpretation. For comparisons, the data in Refs. 3 and 4 must be shifted to the right by one unit.

Our calculations have been performed for a two-dimensional circular quantum dot, solving the Schrödinger equation self-consistently within a mean-field approximation including exchange and correlation effects via a local-density-functional approach.[2,3] The two-dimensional (2D) approximation is appropriate, because the thickness of the quantum dot in the vertical direction is only 12 nm, corresponding to the $In_{0.05}Ga_{0.95}As$ quantum well width,[1] and is therefore significantly smaller than the dot diameter.

The two-dimensional Schrödinger equation for the dot reads, in polar coordinates,

$$-\frac{\hbar^2}{2m^*}\left\{\frac{1}{\rho}\frac{\partial}{\partial\rho}\left[\rho\frac{\partial\psi(\rho,\phi)}{\partial\rho}\right]+\frac{1}{\rho^2}\frac{\partial^2\psi(\rho,\phi)}{\phi^2}\right\}+V(\rho)\psi(\rho,\phi)=E\psi(\rho,\phi), \tag{1}$$

where $\hbar$ is the reduced Planck constant, m^* the effective mass of the electron, ρ the radial coordinate, and ϕ the angular coordinate. The material parameters for $In_{0.05}Ga_{0.95}As$ have been computed with a linear interpolation between the parameters of InAs and GaAs, which gives $m^*=0.0648m_0$ and $\varepsilon_r=12.98$. The total potential $V(\rho)$ includes[3] the confinement potential, the Coulomb interaction term with the other electrons, and the exchange and correlation terms, evaluated on the basis of the polynomial approximations given by Tanatar and Ceperley[8]. The confinement potential is assumed to be parabolic up to a distance corresponding to the geometric dot radius, where hard walls define the outer boundary. Such a potential landscape is consistent, as discussed in the following, with the experimental results for the charging energy.

The 2D Schrödinger equation is separable into azimuthal and radial equations

$$\frac{d^2\Phi(\phi)}{d\phi^2}+\nu^2\Phi(\phi)=0, \tag{2}$$

$$\frac{d^2P(\rho)}{d\rho^2}+\frac{1}{\rho}\frac{dP(\rho)}{d\rho^2}-\frac{2m^*}{\hbar^2}V(\rho)P(\rho)+\left(k^2-\frac{\nu^2}{\rho^2}\right)P(\rho)=0, \tag{3}$$

where ν^2 is the separation constant and $k^2=2m^*E/\hbar^2$. Enforcing periodic boundary conditions, the azimuthal equation has the standard solution $\Phi=c\exp(\pm i\phi)$. For $\nu^2=0$ we have only one solution, while for $\nu^2\neq 0$ there are two solutions corresponding to the up and down orientations of the angular momentum. The radial equation is properly discretized and solved numerically, with a self-consistent iterative procedure.[3]

For a dot radius around 100 nm and a number of electrons around 20, convergence is attained with a few tens of iterations, which take less than a minute of CPU time on a high-performance workstation. For smaller dots, fewer iterations are needed, because the self-consistent problem differs just by a weak perturbation from the single-electron problem, and the iteration procedure converges monotonically to the solu-

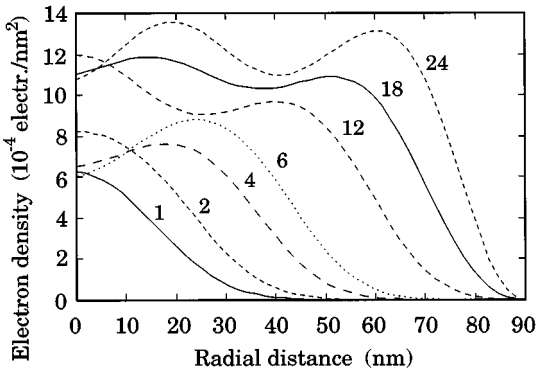

FIG. 1. Electron density as a function of dot radius, for different electron numbers; the geometric dot radius is 90 nm and the confinement potential is parabolic, with $\hbar\omega=3$ meV.

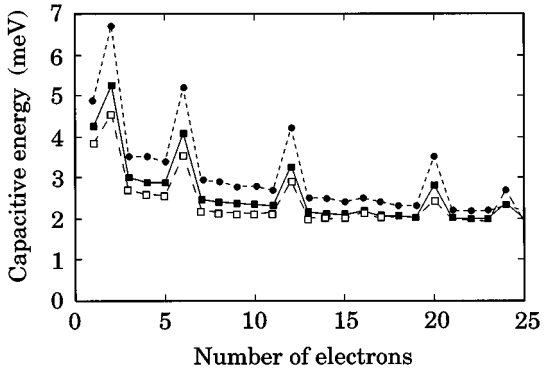

FIG. 2. Self-consistent capacitive energy of a quantum dot with a radius of 90 nm as a function of the number of electrons, including a parabolic confinement potential defined by $\hbar\omega=4$ (solid dots), 3 meV (solid squares), and 2.5 meV (empty squares).

tion. This is the consequence of the fact that the interaction energy scales with $1/R_e$, R_e being the effective radius over which the electron wave function is spread, while the confinement energy scales with $1/R_e^2$.[9] Thus, for increasing dot size, the Coulomb energy becomes more and more important, leading to a very stiff self-consistent problem.

The chemical potential $\mu(N)$, corresponding to the energy needed to add the Nth electron to a system with $N-1$ electrons, is computed by means of Slater's transition rule[2,10], in order to avoid the amplification of numerical errors associated with differentiations.

It is important to clarify that the term ''addition energies'' as used in Ref. 1 is misleading, because the quantity $\Delta\mu$ is actually the equivalent of a classical capacitive energy, i.e., the variation in the dot potential energy as a consequence of the addition of one electron. The properly defined addition energy, i.e. the energy needed to add an electron onto the dot, is just the chemical potential $\mu(N)$. Let us then define the capacitive energy[4] as $e^2/C(N)=\mu(N+1)-\mu(N)$: this is the quantity to be compared with the ''addition energy'' of Ref. 1.

We observe that, after a few oscillations of decreasing amplitude, the measured capacitive energy[1] tends to saturate around a value of 1.25 meV as the number of electrons increases. This effect is due to the varying effective dot radius: for small electron numbers, the effective radius is smaller than the geometrical radius, leading to an increase of the capacitive energy, which, in a semiclassical approximation, is inversely proportional to the radius. For large electron numbers, the size of the dot grows as much as the depletion region due to the side gate permits.

We have computed the electron density for a dot with a geometrical radius of 90 nm and a parabolic confinement potential given by $V_p=1/2m^*\omega^2r^2$, where r is the radial coordinate and $\hbar\omega=3$ meV. The results are presented in Fig. 1 for various electron numbers. One can see that the effective radius starts approaching the geometrical radius only for a number of electrons larger than 18. We have made this choice of parameters because $\hbar\omega=3$ meV corresponds to the estimate given in Ref. 1, and $R=90$ nm is a value allowing quick convergence.

The corresponding behavior of the capacitive energy is shown in Fig. 2 by the solid squares. The other results in Fig. 2 are for dots with the same geometrical radius, but with a confinement potential with $\hbar\omega=4$ (solid dots) 2.5 meV (empty squares).

Examining the detailed features of these results, we notice that peaks occur in more positions than those predicted on the basis of a mere parabolic confinement potential. Each peak in the capacitive energy corresponds to the filling of a ''shell,'' i.e., a set of degenerate orbitals. If one adds an electron to an unfilled shell the capacitive energy is simply due to the increased electrostatic repulsion as for a classical capacitor. Thus it is substantially constant and depends on the dot diameter. When, instead, an electron is added to a different shell, the capacitive energy also includes the variation between the energy eigenvalues associated with the two consecutive shells. For the case of a bare parabolic potential and neglecting electron-electron interactions, there should be peaks at $N=2$, 6, 12, 20, and 30, because each shell accommodates 2, 4, 6, 8, and 10 electrons.[1] In our self-consistent results there are peaks also at $N=16$ and 24. These are due to the fact that the effective self-consistent potential ''seen'' by each electron is not parabolic, and therefore only degeneracies associated with the circular symmetry remain. Each orbital with $\nu=0$ is double degenerate (just the spin degeneracy), while for $\nu\neq0$ we have fourfold degeneracy, as discussed previously. For example, if we look at the data obtained from the self-consistent solution for $\hbar\omega=3$ meV and 24 electrons, the orbitals are ordered (from the point of view of the energy eigenvalues) as follows: (0,1) (1,1) (2,1) (0,2) (3,1) (1,2) (4,1), with the angular and radial quantum numbers indicated by the first and second numbers, respectively. In order to proceed rigorously, we should consider the data for the values of N corresponding to each transition we are interested in, but, for the purpose of exemplification, let us just look at the separation between consecutive energy eigenvalues for $N=24$. We find values around 0.9 meV, except for two cases, that of the pair (2,1)-(0,2), for which the separation is only 0.049 meV, and that of the pair (3,1)-(1,2), for which we have a separation of 0.17 meV. Thus the (2,1) and (0,2) orbitals are almost degenerate (for a parabolic potential they would be exactly degenerate) and this is the reason why no peak is observable in the capacitive energy reported in Fig. 2 for $N=10$. The relatively small separation

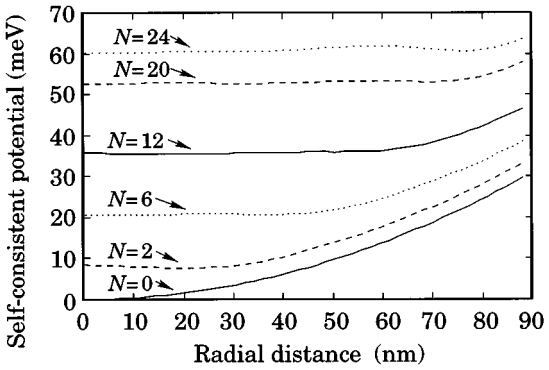

FIG. 3. Self-consistent potential of a quantum dot with a geometrical radius of 90 nm and a parabolic confinement potential defined by $\hbar\omega=3$ meV, for different electron numbers; the potential for $N=0$ corresponds to the bare parabolic confinement potential.

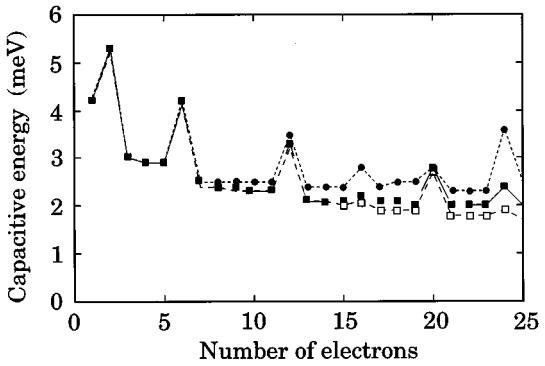

FIG. 4. Self-consistent capacitive energy of a quantum dot including a parabolic confinement potential defined by $\hbar\omega=3$ meV and with a geometrical radius of 75 nm (solid dots), 90 (solid squares), and 120 nm (empty squares).

between (3,1) and (1,2) leads to the reduced peak height for $N=16$. A small peak for $N=16$ is clearly visible in the experimental results of Ref. 1.

The actual shape of the self-consistent potential is shown in Fig. 3 for $\hbar\omega=3$ meV: increasing the number of electrons the potential is gradually flattened out and raised. The presence of a peak for $N=4$ in the experimental data of Ref. 1 may be due to the lack of circular symmetry as a consequence of size fluctuations, or of the presence of an impurity. If the circular symmetry breaks down, the only degeneracy left is that associated with the spin: each shell will accommodate only two electrons, and the capacitive energy will exhibit a peak in correspondence with each even value of N (see Ref. 2). Asymmetry effects do not appear at higher electron numbers, possibly because of screening effects.

Comparing the numerical values of the capacitive energies in Fig. 2 with the experimental data in Fig. 1(b) of Ref. 1, we notice that, up to $N=7/8$ the latter lie somewhere between the curves for $\hbar\omega=2.5$ and 4 meV, while, for larger N, they are definitely lower. Since for small N the best approximation is represented by the curve with $\hbar\omega=4$ meV, and for N around 7 by that for $\hbar\omega=2.5$ meV, the actual bare confinement potential could be best approximated with a somewhat less than quadratic function.

For large values of N, all three curves of Fig. 2 tend to merge to an asymptotic value of approximately 2 meV, as a consequence of the hard walls limiting any further increase of the effective dot size. This value of the charging energy is approximately equal to that (E_{cc}) classically expected for a two-dimensional conducting disk with a radius of 90 nm:[2,11]

$$E_{cc}=\frac{e^2}{8R\varepsilon_0\varepsilon_r}=1.94\ \text{meV}, \tag{4}$$

where R is the disk radius, ε_0 is the vacuum permittivity and ε_r is the relative permittivity of the medium in which the disk is embedded.

This trend toward an asymptotic value depending on the maximum dot size is clearly visible in the results reported in Fig. 4, where the three curves represent the capacitive energies for $\hbar\omega=3$ meV for a dot radii of 75 nm (solid dots), 90 nm (solid squares), and 120 nm (empty squares). For small values of N, for which the effective dot size is not influenced by the distance of the hard walls but only by the profile of the bare parabolic potential, we obtain the same results for all three cases, while, for large values of N, the curves saturate approximately at the classical capacitive energies $E_{cc}=1.45$, 1.94, and 2.32 meV that would be expected for $R=75$, 90, and 120 nm. The curve for $R=120$ nm does not reach the limiting value of 1.45 meV in our plot: this is due to the fact that the number of electrons needed to reach saturation increases with the dot radius.

From the experimental data, we notice that the capacitive energy decreases to about 1.25 meV, which within the classical electrostatic analogy corresponds to a dot radius of 140 nm. This is a reasonable value, considering that the lithographic radius is 250 nm and that a depletion zone must form due to the Schottky contact of the side gate. For values of N larger than those reported in Fig. 1(b) of Ref. 1, the capacitive energy may decrease further, implying an even larger dot radius.

Results of calculations performed for a dot radius of 140 nm and a parabolic confinement potential with $\hbar\omega=2.48$ meV are shown in Fig. 5. Although the slope of the confinement potential has been lowered with respect to the curves of Fig. 4, the capacitive energy does not reach the expected

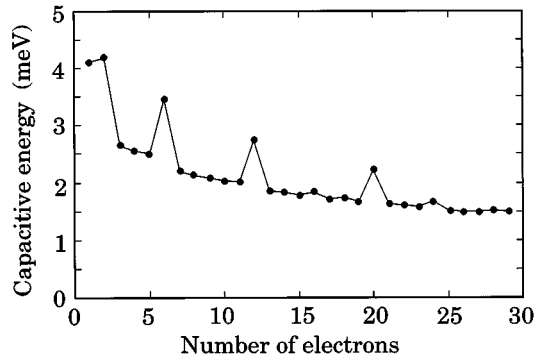

FIG. 5. Self-consistent capacitive energy in a quantum dot including a parabolic confinement potential defined by $\hbar\omega=2.48$ meV, and with a geometrical radius of 140 nm.

saturation value of 1.24 meV even for 30 electrons. Calculations for larger dots and/or for smaller values of $\hbar\omega$ are very difficult, because of numerical convergence problems.

In summary, we presented a numerical simulation of the capacitive charging energy of a model quantum dot which agrees well with recently found experimental results. Our model explains peaks in the capacitive energy found in addition to those predicted for a mere parabolic confinement potential. Furthermore, we derived estimates for the shape of the confinement potential and the maximum radius of the quantum dot.

We thank Leo Kouwenhoven for providing us with an unpublished version of the experimental results and useful discussions. This work received partial support from the NATO Collaborative Research Grant No. 950753. M. M. also acknowledges support from the Italian Ministry of the University and Scientific Research, and K. H. support from the Army Research Office.

[1] S. Tarucha, D. G. Austing, T. Honda, R. J. van der Hage, and L. P. Kouwenhoven, Phys. Rev. Lett. **77**, 3613 (1996).

[2] M. Macucci, Karl Hess, and G. J. Iafrate, Phys. Rev. B **48**, 17 354 (1993).

[3] M. Macucci, Karl Hess, and G. J. Iafrate, J. Appl. Phys. **77**, 3267 (1995).

[4] G. J. Iafrate, K. Hess, J. B. Krieger, and M. Macucci, Phys. Rev. B **52**, 10 737 (1995).

[5] S. Tarucha, D. G. Austing, and T. Honda, Superlattices Microstruct. **18**, 121 (1995).

[6] D. G. Austing, T. Honda, and S. Tarucha, Semicond. Sci. Technol. **11**, 388 (1996).

[7] J. Weis, R. J. Haug, K. v. Klitzing, and K. Ploog, Phys. Rev. B **46**, 12 837 (1992).

[8] B. Tanatar and D. M. Ceperley, Phys. Rev. B **39**, 5005 (1989).

[9] G. W. Bryant, Phys. Rev. Lett. **59**, 1140 (1987).

[10] J. P. Perdew and Alex Zunger, Phys. Rev. B **23**, 5048 (1981).

[11] L. P. Kouwenhoven, N. C. van der Vaart, A. T. Johnson, W. Kool, C. J. P. M. Harmans, J. G. Williamson, A. A. M. Staring, and C. T. Foxon, Z. Phys. B **85**, 367 (1991).